The Combined Role of ENSO-driven Sea Surface Temperature Variation and Arctic Sea Ice Extent in Defining Climate Conditions in the Southwestern United States

Amanda M. Chassot

Thesis submitted to the faculty of the Virginia Polytechnic Institute and State University in partial fulfillment of the requirements for the degree of

Master of Science
In
Geosciences

J. O. Sewall, Chair
J. E. Barrett
E. R. Kraal
J. A. Spotila

June 10, 2009
Blacksburg, Virginia
Keywords: Little Ice Age; ENSO; Arctic sea ice; climate change

The Combined Role of ENSO-driven Sea Surface Temperature Variation and Arctic Sea Ice Extent in Defining Climate Conditions in the Southwestern United States

Amanda M. Chassot

(ABSTRACT)

Previous research indicates that future reductions in Arctic sea ice cover (SIC) could alter storm tracks and precipitation patterns in western North America and negatively impact water resources in the American southwest. Other research suggests that multiple periods of increased precipitation and/or cooler temperatures in the American southwest during the Little Ice Age (LIA) were due to strong El Niño events; historical records also describe expanded Arctic SIC at this time.

We use 16th-19th century Arctic SIC records from the ACSYS Historical Ice Chart Archive as a basis for expanding Arctic SIC from 1870 HadISST data to theoretical LIA extents. Then, in a suite of sensitivity studies, we investigate the relative influences of and interactions between El Niño-Southern Oscillation (ENSO) related sea surface temperature (SST) variation and varying Arctic SIC in controlling storm tracks, precipitation patterns, and overall climate conditions in the American southwest.

We find that tropical Pacific SSTs greatly influence climate system response to variability in Arctic SIC, with ENSO-Neutral SSTs permitting the greatest response. Additionally, the degree of expansion and symmetry of Arctic SIC also influence precipitation regime response. These findings suggest that the climate response to future Arctic SIC retreat may not only be highly dependent on the spatial patterns and extent of SIC reductions, but also upon ENSO variability, such that El Nino events may reduce the potential climate impact of ice reductions as compared to Neutral or La Nina events

Table of Contents

Tables

Figures

Introduction

Variability and changes in climate affect the availability and sustainability of water resources [*Gleick and Adams,* 2000]. The American Southwest is particularly vulnerable to water stress due to the arid climate and increasing population [*Perry and Mackun,* 2001]. Winter storms account for a significant proportion of annual precipitation in the western United States, and even in the areas that receive summer monsoon precipitation, 30% of annual precipitation can be attributed to winter storms [*Barry and Chorley,* 1998; *Sheppard et al.,* 2002]. The soaking rains at lower elevation and snowfall in the mountains during winter provide important inputs to the regional water budget [*Winograd et al.,* 1998]. The slow release of water from snowmelt can be more effective than an equal amount of rain because a larger proportion of the water in snow will be translated into plant-available water [*Loik et al.,* 2004].

There are multiple controls on winter precipitation in the Southwest, including the El Niño-Southern Oscillation (ENSO) and Arctic sea ice extent. During El Niño, the warm phase of ENSO, warm water in the eastern Pacific provides the energy to develop troughs along the west coast of the United States and mid-latitude winter storms are displaced southward, leading to an increase in precipitation penetrating into the American Southwest. This additional precipitation can have large effects on the arid southwest, and many southwestern basins are at least 10 times as likely to have anomalously high flows during El Niño events than during La Niña events [*Cayan et al.,* 1999]

Additionally, changes in Arctic sea ice extent can affect mid-latitude climate through storm-track shifts which alter precipitation regimes. Magnusdottier et al. [2004] identified a hemispheric response to changes in sea ice extent in the North Atlantic reflected in changes in geopotential height and storm tracks, and they found that sea ice anomalies in the North Atlantic were more efficient at exciting an atmospheric response than sea surface temperature (SST) anomalies. Additionally, summer ice extent may exert some control over winter climate. Francis et al [2009] found a stronger geopotential height gradient (1000 to 500 hPa) in winters that were preceded by summers with greater

ice cover than those preceded by low-ice cover summers; a stronger gradient supports a stronger polar jet stream and semi-permanent low pressure centers, which in turn affect storm tracks and intensity. Shifting storm tracks results in altering precipitation regimes and can affect annual water budgets [*Sheppard et al.*, 2002]. As Arctic sea ice extent continues to decrease, it is likely that there will be changes in storm tracks and precipitation patterns that will lead to increased water stress in the American west. Modeling studies of future reductions of Arctic sea ice show a northward shift in mid-latitude winter storm tracks, effectively drying southwestern North America [*Sewall and Sloan*, 2004; *Sewall*, 2005; *Singarayer et al.*, 2006]. However, variability in winter precipitation in the Southwest is more often attributed to other modes of variability, such as the Pacific Decadal Oscillation, the Pacific North America Pattern, and ENSO [*Sheppard et al.*, 2002]. A better understanding of how different natural forcings (e.g. ENSO and Arctic sea ice cover) can modulate precipitation in the southwest on multi-decadal timescales may provide valuable insight into future predictions of water availability in the southwest.

The extent to which ENSO and sea ice interact to influence southwestern precipitation can be investigated within the framework of the Little Ice Age (LIA). The LIA was a period of time ca.1450 to 1850 A.D in which global temperatures were slightly cooler (~0.5C) [*Bradley and Jones*, 1992; *Grove*, 1988; *Lamb*, 1976] and many glaciers expanded to more advanced positions than today [*Grove*, 1988]. There are historical records of increased North Atlantic sea ice (Brink Løyning, 2003) and evidence of ENSO variability or persistent El Niño states during the LIA [*Cobb et al.*, 2003; *D'Arrigo et al.*, 2005; *Mann et al.*, 2005]. This historical, documented climate event demonstrates that small shifts in climate forcing factors can have significant regional and global impacts. Thus, the LIA can provide a frame of reference for investigating how small changes in surface forcing, such as through changes in Arctic sea ice extent or shifts in tropical Pacific SSTs, can affect climate.

ENSO is believed to have greatly impacted southwestern precipitation during the Little Ice Age, during which the North Atlantic also experienced periods of greater sea

ice extent than modern day [*Brinck Løyning et al.*, 2003]. Historical and early instrumental data have recorded the effects of the LIA in Europe, but documentation is lacking in other parts of the world. However, proxy evidence provides a case for greater climate variability in western North America during the LIA, as southwestern North America experienced greater precipitation in the LIA than during modern times [*Herweijer et al.*, 2006]. There is evidence that anomalous precipitation in the southwest may be linked to frequent or persistent El Niño events; coral records analyzed by Cobb et al [2003] express greater frequency and amplitude of ENSO activity in the 17th century than in the late 20th century. In addition, D'Arrigo and Jacoby [1991] identified decadal scale wet/dry periods in New Mexico during the last 1000 years, which includes both sustained drought and periods of high precipitation during the Little Ice Age (dry: 1778 – 1787, wet: 1609-23, 1835-49). Two of the four wettest individual years that they identified (1720, 1816) occurred during the LIA and correspond to El Niño events [*D'Arrigo and Jacoby*, 1991].

Arctic sea ice extent has also been cited as a factor in altering precipitation regimes in the western United States, with reductions in sea ice being linked to northward trending storm tracks leading to regional drying in the desert southwest [*Sewall and Sloan*, 2004; *Sewall*, 2005; *Singarayer et al.*, 2006]; therefore, increased sea ice, such as during the LIA, may be conducive to more southerly storm tracks, which could contribute to the documented increases in precipitation in the desert southwest [*Herweijer et al.*, 2006]. The combined influence of tropical Pacific SSTs and Arctic sea ice on precipitation and storm track variability in the southwestern United States can be explored via the comparison of Little Ice Age Arctic sea ice conditions to the modern day under different ENSO phases, and will provide insight into how these factors interact in defining winter precipitation and storm tracks in the Southwest. Here, we present our findings that ENSO phase plays a role in modulating the potential influence of changes in Arctic ice extent, and that the symmetry/location of sea ice anomalies also influences the system response to increased sea ice.

Methods

In order to investigate the effects of expanded Arctic sea ice and ENSO-related SST variability on precipitation and storm tracks in the southwestern United States, we developed a suite of fixed annual-cycle SST and sea ice, atmosphere-only simulations representing modern and Little Ice Age Arctic sea ice conditions. Each simulation was forced with one of two possible LIA Arctic sea ice annual cycles and one of three SST scenarios (strong El Niño, strong La Niña, or ENSO-Neutral).

We use 15th to 19th century Arctic sea ice extent/concentration records from the ACSYS Historical Ice Chart Archive [*Brinck Løyning et al.*, 2003] and maximum spring pack ice extent in the North Atlantic proposed by Lamb [1963] to define spring maximum and fall minimum Arctic Sea Ice extents in the North Atlantic. As records of the Arctic ice edge are often limited to small portions of the North Atlantic sector of the Arctic we assembled a theoretical maximum sea ice extent in the Labrador, Greenland, Norwegian, Barents, and Kara seas from multiple year records with the greatest ice extent in some part of the North Atlantic (1787,1798,1812,1816). We expanded 1°x1° 1870 HadISST Arctic Sea Ice data [*Rayner et al.*, 2003] to approximate these observation-based North Atlantic extents in ArcGIS using the kernal density function at a radius of 12 cells and manually edited the ice grid to constrain ice coverage to our defined maximum extent. Because Pacific sea ice extent during the LIA has not been defined to a similar resolution the ice in the North Atlantic, we developed two Arctic sea ice grids. In the asymmetrical grid (AS-LIA), Arctic sea ice located between 130° and 245° longitude was replaced with HadISST 1870 maximum sea ice values, to constrain Arctic Sea ice through the Bering Strait to historical 1870 values. In the symmetrical grid (LIA-), sea ice in the Pacific was expanded concurrently with the North Atlantic ice, using the same parameters. GIS data was exported and converted to NetCDF grids.

An inherent problem with expanding the ice using a density function is that the slope of the gradient from 100% - 0% ice becomes unrealistically low. By applying the function

$$\text{icefraction} + 3\left[\left(100 - \text{icefraction}\right) \times \sin\left(\frac{\text{icefraction}}{\pi 100}\right)\right] + 0.5\left[\left(100 - \text{icefraction}\right) \times \sin\left(\frac{\text{icefraction}}{\pi 100} - \frac{1}{\pi}\right)\right]$$

to both grids, the gradient was artificially steepened better reflect the natural gradation between core and edge of the ice pack.

A similar process was used to develop an annual minimum Arctic ice extent, using ice from 1693, 1749, 1769, 1800, 1818, and 1819. Values from 1910 & 1911 were used where LIA data were not available. We defined monthly distributions between the two extremes using a sine to complete the annual cycle. Our Modern sea ice scenario (MOD) was defined using mean ice values from HadISST from the years of 1971-2000. Southern Hemisphere sea ice values for all three ice grids were set to monthly HadISST 1870 values.

We used monthly 1971 – 2000 Multivariate ENSO Indices (MEI) [*Wolter and Timlin*, 1993; 1998] to select the strongest El Niño or La Niña years to create global SST grids representing maximum El Niño or La Niña annual cycles. Strong years were determined as calendar years in which at least one monthly MEI value was >1 SD (El Niño) or <-1 SD (La Niña). The greatest (least) SST value for each cell was then used to create maximum El Niño (La Niña) SST distributions. Average values from calendar years with all reported MEI values between -1 and 1 SD were used to create an ENSO-Neutral SST grid.

We combined these three Arctic sea ice grids (MOD-, LIA-, AS-LIA-) and three SST grids (Neutral, El Niño, La Niña) to create nine scenarios. Table 1 shows the combinations of sea ice and SST grids which define forcing conditions for the six experimental and three control scenarios.

We ran these nine scenarios (table 1) as 30-year fixed SST/sea ice, atmosphere only, experiments using the NCAR Community Atmosphere Model 3.0, (CAM3), (Collins et al 2006) at a T42 (~2.8° latitude x ~2.8° longitude) spectral resolution. Atmospheric carbon dioxide concentrations were set to pre-industrial levels (280 ppm); CFCs were set to 0; and orbital parameters were set to the initial year 1870. All other initial boundary conditions were set to standard default values. We used monthly averages of the final decade of each 30-year run for analysis and comparison.

	Sea Ice Extent		
SST	Modern	LIA	AS-LIA
ENSO-Neutral	*Modern-Neutral*	*LIA-Neutral*	*AS-LIA-Neutral*
El Nino	*Modern-Nino*	*LIA-Nino*	*AS-LIA-Nino*
La Nina	*Modern-Nina*	*LIA-Nina*	*AS-LIA-Nina*

Table 1: Experimental Design

Results

Winter precipitation accounts for 30% of annual precipitation in Arizona and New Mexico [*Barry and Chorley*, 1998], the majority of annual precipitation in southern California [*Legates and Willmott*, 1990], and is hydrologically important throughout the western states [*Bryson and Hare*, 1974; *Sheppard et al.*, 2002] as snowmelt provides the majority of water recharge in many areas [*Winograd et al.*, 1998]. Winter is also the season during which El Niño has the greatest influence on storms and precipitation penetrating into the southwest. Therefore, we focus our analyses on ten-year winter season (December, January, February; DJF) averages of 500 mb geopotential height (Z_{500}), 850 mb meridional heat transport (VT_{850}), total precipitation (P_T), and evaporation minus precipitation (E-P) with results from experimental simulations (LIA, AS-LIA) compared to the control simulation (MOD) across each ENSO SST condition (Neutral, Niño, Niña). Unless otherwise noted, results discussed below are differences in winter conditions between LIA or AS-LIA and MOD sea ice forcing. All differences are across similar ENSO phase conditions (e.g. LIA-Niño minus MOD-Niño).

While differences in Z_{500} were analyzed for the entire northern hemisphere, other variables were examined for a region bounded by (65°N, 165°W) and (25°N,100°W) that includes most of western North America and the northeastern Pacific Ocean (see figures 2-4; hereafter referred to as western North America) and also for a 23 grid cell southwestern U.S.A. region (see bounding box in figures 2-4 hereafter referred to as the desert southwest). We performed paired t-tests at the α=0.05 significance level (Fisher 1925) for hemispheric Z_{500}, and also for P_T and E-P in the southwestern region to examine the significance of differences in atmospheric structure and moisture variables. Additionally, proportional differences between experimental and control conditions were calculated for each cell as: (experimental_cell - control_cell)/control_cell, summed, and then averaged over the region of interest (Northern hemisphere, western North America, or desert southwest) and reported as percent change for comparison of the relative direction and magnitude of changes induced by our imposed LIA or AS-LIA sea ice forcing.

Significant (two-tailed, α =0.05) differences in Z_{500} were seen throughout the northern hemisphere (figure 1a-f) in response to increased LIA and AS-LIA Arctic sea ice for all simulations, except for LIA-Niño. Both LIA and AS-LIA simulation results show reductions in Z_{500} over the North Pole as compared to MOD. LIA-Neutral shows the largest reductions in Z_{500} over the North Pole (~10 m) (figure 1a). AS-LIA-Neutral (figure 1d) produces a similar, symmetrical pattern of differences as LIA-Neutral, when compared to MOD, but the magnitude of change is much smaller, with maximum decreases of approximately 6 m. Both Neutral SST simulations only show small increases in Z_{500} (~1-2 m) through the mid-latitudes. AS-LIA-Niña (figure 1f) and LIA-Niña (figure 1c) have high-latitude Z_{500} reductions of ~7 m, with the anomaly approximately centered over the Barents and Kara seas; small increases (<5 meters) in Z_{500} are seen over portions of the Atlantic Ocean between 30°N and 55°N and the Pacific Ocean south of 55°N, with greater increases seen in LIA-Niña than AS-LIA-Niña. Differences in Z_{500} under El Niño conditions (figure 1b, d) are of smaller magnitude than under other SST conditions and there is no cohesive response in the area of greatest ice forcing; however, we do see reductions of ~2-4 meters over North America and increases of ~2-4 meters over Europe and the Pacific Ocean, with the relatively stronger decreases in AS-LIA-Niño, and the relatively greater increases in LIA-Niño.

As a proxy for storm activity, we compare 850 mb meridional heat transport (VT_{850}) under the varying SST and sea ice conditions. As VT_{850} represents meridional heat transport at the 850 mb pressure surface, 20 cells in the western North America region (8 in the desert southwest sub-region) are missing values due to topography. These cells were excluded from calculations. VT_{850} differences over the western North America region indicate changes in storm activity in all simulations, but the intensity and direction of change vary considerably (figure 2a-f). Proportional changes were calculated as: abs((experimental_cell - control_cell)/control_cell) and then summed and averaged to determine regional absolute percent change in storminess.

With the increased Arctic sea ice, absolute proportional changes in VT_{850} in western North America are of similar magnitude in AS-LIA-Niño (~39%), AS-LIA-Niña (~44%), AS-LIA-Neutral (~47%) , and LIA-Niña (~50%). Smaller absolute changes are seen in LIA-Niño (~24%). The largest changes are seen in LIA-Neutral (~147%).

Looking at changes in VT_{850} over the desert southwest (highlighted area within figure (figure 2a-f) we see the greatest absolute proportional changes in VT_{850} in LIA-Neutral (figure 2a) and AS-LIA Neutral (figure 2d) at 323% and 126%, respectively, compared to MOD storm activity. Additionally, VT_{850} changes for AS-LIA Niño (figure 2e, 121%), LIA-Niña (figure 2c, 57%), and LIA-Niño (figure 2b, 35%) are also larger within the desert southwest than for Western North America at-large while absolute proportional VT_{850} change in AS-LIA-Niña (figure 2f, 42%) is similar to the average change in Western North America.

P_T differences were compared for western North America, and both PT and E-P differences were compared for the desert southwest for experimental and control conditions. While precipitation increases over large regions of western North America under the increased sea ice conditions (both AS-LIA and LIA), the location of precipitation changes varied substantially between simulations. P_T increased for western North America with increased sea ice for both LIA-Neutral (13%) and AS-LIA-Neutral (18%) simulations (figure 3a,d). However, while El Niño results show increases in the Pacific Northwest, PT for Western North America decreased by ~4% and ~5% for LIA-Niño and AS-LIA-Niño, respectively (figure 3b,e). LIA-Niña (figure 3c) showed modest P_T increases (4%) and AS-LIA-Niña (figure 3f) had reductions of similar magnitude (-4%) when compared to MOD.

For precipitation in the desert southwest, the greatest significant increases occurred under LIA-Neutral (figure 3a, $p < 0.001$) and AS-LIA-Neutral (figure 3d, $p < 0.001$), with increased precipitation in every grid cell, and with more than half of LIA-Neutral desert southwest grid cells and ¼ of AS-LIA-Neutral desert southwest grid cells experiencing >25% increases in winter precipitation as compared to MOD-Neutral conditions. While

in all simulations there are individual southwestern cells with increased precipitation compared to MOD conditions, both El Niño (figure 3b,e) and La Niña (figure 3c,f) simulations showed an average decrease in precipitation in the desert southwest; under El Niño SST conditions, significant decreases in P_T occurred for the desert southwest, -4% in LIA-Niño ($p=0.023$), and -11% in AS-LIA-Niño ($p=0.014$). Both La Niña simulations did not yield significant results when compared to MOD.

The overall moisture budget of the desert southwest is represented by the quantity evaporation-precipitation (E-P). Figure 4a-i shows actual E-P values for control and experimental conditions. Average proportional change for each cell was calculated as (ctrl_cell-exp_cell)/abs(ctrl_cell), then all desert southwest proportional change values were summed, averaged and then reported as average percent change for the desert southwest. E-P paired T-test results for the desert southwest show significant moisture increases over MOD conditions in LIA-Neutral ($p < 0.001$, 64%), and AS-LIA-Neutral ($p < 0.001$, 40%). LIA-Niño ($p=0.047$, 3%) and AS-LIA-Niña ($p < 0.001$, 25%) had significantly less moisture than their MOD counterparts. No significant E-P changes occur in AS-LIA-Niño and LIA-Niña.

Discussion

This study investigates how variations in ENSO-phase and Arctic sea ice extent interact to impact climate in the desert southwest. We find that these sources of variability interact such that ENSO-phase modulates the degree to which increased Arctic sea ice extent can affect climate. Under ENSO-Neutral SST's and increased Arctic sea ice, the desert southwest experiences an increase in winter precipitation ranging from 5% to greater than 50% , and these changes in precipitation can be attributed to the shifting of winter storm tracks. Under increased sea ice conditions, the largest relative increases in storm activity and precipitation in the desert southwest occur under ENSO-Neutral SST conditions (figures 2a, 3a), with smaller relative increases seen under La Niña SST conditions (figures 2c, 3c). Very few significant changes were seen under El Niño SST conditions (figures 2b, 3b). Precipitation increases throughout the desert southwest under ENSO-Neutral conditions with some areas within the region receiving a greater than 40% increase in winter precipitation (figure 3a,d). However, both increases of smaller magnitude (<40%) and reductions in winter precipitation are seen under El Niño and La Niña SST conditions (figure 3b,c,e,f). It is reasonable to expect that increased precipitation would be associated with changes in storm activity. This is supported by absolute proportional change in VT_{850}, which, in the desert southwest, follows a similar pattern to precipitation in which ENSO-Neutral SSTs contributed to the greatest changes under increased sea ice conditions (figure 2a,d). LIA-Niño, LIA-Niña, and AS-LIA-Niña had changes of much smaller magnitude (figure 2b,c,f). AS-LIA-Niño had a large absolute proportional change in VT_{850} (figure 2e). However, these changes did not extend to increasing precipitation in the desert southwest, as both the largest VT_{850} changes and the only precipitation increases occurred in grid cells along the California coast indicating highly localized changes in storminess that exclude much of the southwest.

The differences in system response to increased Arctic sea ice cover under the various SST scenarios raises the question: how does the ENSO phase modulate the response to a given ice forcing? Colder Arctic surface conditions under expanded ice cover promote

regional lowering of the 500 mb geopotential height (figure 1a-f). Lowered geopotential height in the northern high latitudes steepens the hemispheric geopotential height gradient (figure 5a-f). In these experiments, our positive ice anomaly enhances this gradient, and the steeper gradient creates a greater relative intensity between highs and lows. Additionally, the steeper Z_{500} gradient represents a change in atmospheric structure, which can alter storm activity via its influence on the polar jet stream. The polar jet, a high-altitude air current, significantly influences storm tracks in the mid-latitudes and winter circulation patterns in Western North America as its variable strength and location steer cyclonic systems [*Jorgensen and Klein*, 1967; *Sheppard et al.*, 2002]).This alteration of the geopotential height gradient is similar to Francis et al. [2009], who discuss the relaxation of the regional/hemispheric geopotential height gradient in response to projected reductions in Arctic sea ice. Through the general reduction of the geopotential height gradient, the relative intensity of semi-permanent highs/lows are also reduced, which alters seasonal weather patterns [*Francis et al.*, 2009]

In our six simulations, this steepening of the geopotenial height gradient varies considerably under each of the ENSO-phase SST conditions. The ability of increased sea ice extent to alter atmospheric structure is greatest in the ENSO-Neutral scenario, and the smallest changes in atmospheric structure due to increased ice occur under El Niño SSTs. ENSO-Neutral conditions produced the largest changes in precipitation for the southwest, and these conditions also support the greatest steepening of Z_{500} (figure 5a). El Niño Z500 gradients do not vary, and La Niña conditions produce a gradient steepening that falls between those of ENSO-Neutral and El Niño scenarios (figure 5b,c). The greatest steepening of the Z_{500} gradient, as compared to MOD, occurs in LIA-Neutral (fig 5a), with a steepening of 12% between 0^{o}-90^{o}N , with a smaller 4% steepening in LIA-Niña (fig 5c), and differences are slight in LIA-Niño (<1%) (fig 5b).

Under MOD-Niño, the Z_{500} gradient is the least steep of all three MOD simulations. In terms of large scale atmospheric circulation, there appears to be a more zonal flow throughout the Northern hemisphere, which would encourage the polar jet to have less north/south deviation than the other MOD simulations. The pre-existing symmetrical,

zonal conditions occurring under the LIA-Niño simulation may contribute to the weak response to our ice forcing. The greater alteration of the Z_{500} gradient seen in LIA-Neutral and LIA-Niña simulations relates well to the greater degree of changes in precipitation and storm activity in those simulations.

Similar relationships between the degree of Z_{500} gradient steepening and SSTs occur in AS-LIA simulations (figure 5d-f); however, the gradient alteration differs in the Neutral and La Niña AS-LIA simulations as compared to each corresponding LIA simulation. The minimal change in Z_{500} gradient under LIA-Niño was not significant, but AS-LIA-Niño does show a slightly larger and significant, steepening of its Z_{500} gradient, and has greater responses of southwest precipitation and VT_{850} to increased sea ice. The AS-LIA simulations do maintain the relationship exhibited by the LIA simulations in which gradient change is greatest with Neutral SSTs and least with El Niño SSTs. In AS-LIA simulations, the changes in precipitation and storms in both the Western North America and desert southwest are generally similar, but show regional variation from those occurring in the LIA simulations. This is likely due to the differing gradient response.

The symmetry of the ice anomaly influences the Z_{500} gradient, and while sea ice extending into the Bering Strait is only a small spatial component of total sea ice cover, it significantly contributes to the total influence of Arctic sea ice on atmospheric structure, and ultimately storms and precipitation. Additionally, the relative asymmetry of ice may play a role when atmospheric flow is more zonal, as AS-LIA-Niño produced significant changes in Z_{500} gradient when LIA-Niño did not.

Generally under ENSO-Neutral SSTs, increased sea ice leads to widespread increases in precipitation in the desert southwest. However, precipitation increases in LIA-Neutral (figure 3a) are greater than AS-LIA-Neutral (figure 3d) throughout the southwest, with increases of 10% to 50%+ under LIA-Neutral and increases in AS-LIA-Neutral are typically below 40%. Both of these Neutral simulations also show large-scale changes VT850, which indicates more storm energy being moved into western North America.

However, LIA-Neutral still has a larger magnitude of change than AS-LIA-Neutral, relating to the degree of change in Z_{500} gradients.

Additionally, the two El Niño SST simulations precipitation patterns in response to increased sea ice also have similarities; in both the LIA-Niño and AS-LIA-Niño simulations, we see winter precipitation increases in the Pacific Northwest and central Canada, with a general drying occurring in the southwest; and in VT_{850}, we see increases only in the regions of the SW that also receive additional precipitation due to the sea ice increase. Change in the El Niño experimental simulations are generally of a smaller degree than the other ENSO-phase experiments, and the experiment with significant changes in Z_{500} gradient, AS-LIA-Niño, exhibits larger changes in precipitation and storminess.

The La Niña SST simulations produced the least similar precipitation response to increased sea ice; in the LIA-Niña simulation, decreases are seen through southern California and modest increases (<25%) occur in the Sonoran desert and west Texas. Under AS-LIA-Niña, precipitation increases by 5% - 18% in southern California and parts of the Lower Colorado river basin, but decreases by more that 10% in the Sonoran Desert and west Texas. Only small changes in precipitation are seen in the rest of Western North America under LIA-Niña conditions, but AS-LIA-Niña produces increases in the Pacific Northwest and into the northern Great Plains. Both LIA-Niña (figure 2c) and AS-LIA-Niña (figure 2f) feature large changes in storm activity off of the southern coast of Alaska and penetrating inland to the north. However, these changes are centered close to the western Canadian coast in LIA-Niña, and in AS-LIA-Niña, there are more widespread large magnitude changes in VT_{850}centered near 50ºN directly south of Alaska. These differences extend into the southwest where very different patterns of precipitation changes occur, as discussed above. The same relationship between location/magnitude of VT_{850} changes and increased precipitation in the desert southwest seen in LIA-Neutral exists in both of these simulations, and the magnitude of change for both is smaller than their corresponding Neutral SST counterparts.

Evaporation minus precipitation (E-P) values represent overall moisture budget, and particularly in arid climates, changes in the relationship between evaporation and precipitation in a region have the potential to alter water availability, even without significant changes in precipitation received. The E-P results (figure 4a-i) indicated significant changes in moisture for the desert southwest in most simulations, excluding AS-LIA-NIÑO and LIA-Niña. Both Neutral simulations (figure 4a,d) show increases in available moisture throughout the desert southwest, largely due to the widespread precipitation increases (figure 3a,d). LIA-Niño (figure 4b) and AS-LIA-Niña (figure 4c) both show significant reductions in moisture, but within sub-regions of the desert southwest in these simulations, the degree of reduction in precipitation (10-18%) greatly exceeds the reduction in moisture availability defined by E-P (<5%). This effectively means that even though precipitation is reduced by more than 10%, the net reduction in moisture is less than half of that amount. This suggests that while some grid cells did not experience significant increases in precipitation, there may still be greater water availability at the surface than there would be under modern conditions, due to a relative reduction in evaporation.

For the desert southwest, the Little Ice Age involved greater climatic variability [*Briffa and Jones*, 1991; *Briffa*, 2000] and it also contained some of the most anomalously wet and dry multi-year periods of the past two millennia [*Salzer and Kipfmueller*, 2005]. Hildago et al [2004] found that between 1650 and 1850 dry/wet variability followed a periodicity of 8 to 32 years., Both before and after that time, these cycles have occurred on a longer, 32 to 64 year cycle [*Hidalgo*, 2004]. D'Arrigo and Jacoby's (1991) identification of decadal scale periods of wetter/drier conditions in New Mexico during the LIA lend additional support that the major forcing contributors to LIA climate in the southwest had high-frequency variability. Additionally, Cobb [2003] suggests greater ENSO variability in the 17th century than in the 20th. Our simulations suggest that climate conditions in the southwest during the LIA may also, in part, be due to variability in Arctic ice extent and symmetry.

Expanded sea ice, such as there was during the LIA, can increase the storm activity within and precipitation received by the desert southwest (Fig 2,3). However, the ability of ice forcing to influence climate response is highly dependant on both ENSO phase and ice symmetry. During the LIA, annual sea ice minima and maxima were greater than at present, but there was still year-to-year variability [*Brinck Løyning et al.*, 2003]. Our increases in annual sea ice area represent only two of many possible annual ice distributions, both of which produced different climate responses in the northern hemisphere, which significantly altered precipitation and storms within the desert southwest. While ENSO-Neutral SSTs contributed to region-wide increases in precipitation in the desert southwest, under La Niña and El Niño SSTs we observed some localized increases in winter southwestern precipitation under LIA ice conditions that corresponded to reductions in the same location under the AS-LIA ice conditions, and vice versa (figure 3b,d,e,f). This demonstrates that the symmetry of the Arctic sea ice can influence precipitation patterns within small regions and can contribute to climatalogical variability on shorter time scales than some other modes of variability with longer periodicity, which is consistent with the shorter periodicity of LIA dry/wet cycles identified by Hildago et al [2004].

Additionally, increased Arctic sea ice altered the relationship between evaporation and precipitation in the desert southwest. Even without large increases in precipitation, some locations were able to maintain moisture availability via reduced evaporation (Fig 4a-f), likely due to cloudiness or local temperature variations. El Niño events bring more precipitation to the desert southwest than the other phases of ENSO, and even though ice forcing did not have a significant effect on our El Niño simulations, these simulations still produced the wettest southwestern conditions as compared to the other phases (not shown). However, altering the relationship between evaporation and precipitation in the desert southwest affects the moisture available in this arid region. Under Neutral and La Niña SST conditions, the southwest, during the LIA, may have experienced additional buffering from drying/drought via decreased evaporation and increased precipitation during these drier ENSO-phases.

High frequency or high intensity El Niño events were important contributors to total moisture in the southwest during the LIA, and may have contributed to the development of pluvials in the western United States during the Little Ice Age [*Castiglia and Fawcett*, 2005]. However, the relative increases in precipitation due to increased Arctic sea ice in our ENSO-Neutral simulations and the localized increases in La Niña simulations suggest that increased Arctic sea ice contributed to maintaining relatively wetter conditions by increasing average available moisture. Thus, expanded sea ice cover may also have played a role in developing and maintaining pluvials in non El Niño years via increasing precipitation or reducing the relative evaporation of surface water during the other (drier) phases of ENSO.

The LIA and AS-LIA Arctic sea ice scenarios developed for these simulations were based upon historical records of actual ice variability in the 16th through 19th centuries, and while they represent respective increases of 47% and 36% over MOD, the average increase in ice extent in the North Atlantic is only ~3.5^{o} latitude, or an average increase of ~500 km along a particular line of longitude in the North Atlantic.

The differences in the system response between the two ice scenarios (see e.g. Fig 1,2,3) suggest that not only ice extent/area, but also ice symmetry and location of increases are all large contributors to response, both on the regional and hemispheric scale. While examining 20th century ice variability, Deser et al. [2000] found a connection between ice variability in the Greenland Sea and the number of cyclones occurring east of Greenland in the vicinity of the climatological mean Icelandic low. However, our changes in ice forcing were located far from our region of interest, the desert southwest, which was significantly influenced by our imposed Arctic ice increases. While changes in sea ice can have significant effects on adjacent regions, this work further supports the findings that Arctic surface forcing can have mid-latitude climate implications through its influence on atmospheric structure. Additionally, these changes do not have to be widespread or particularly large in magnitude. Focused, more localized variations in ice symmetry or ice extent can have far field effects, such that locations of change in sea ice spatial extent may be equally important to the magnitude of ice extent change.

Perennial Arctic sea ice cover has been steadily declining during the late 20th and the 21st century [*Comiso,* 2002; *Comiso et al.*, 2008]. There have been predictions that annual ice cover may be reduced by up to 46% by 2050 [*Walsh and Timlin,* 2003] and that by 2100, the Arctic could be 95% ice free during the summer [*Smedsrud et al.*, 2008]. Holland et al. [2006] discuss observed and modeled abrupt reductions in sea ice, expressing a rapidly increasing rate of ice retreat under some prediction models, particularly without the reduction of greenhouse gas emissions.

With Arctic sea ice decline, some researchers have predicted a drier American southwest [*Sewall and Sloan,* 2004; *Sewall*, 2005; *Singarayer et al.*, 2006] due to the ice influence on storm tracks. However, climatological precipitation controls for the southwest are still not fully understood. Woodhouse and Meko [1997] expressed that ENSO-PNA (Pacific North American) patterns and the Southwest Low pattern explain winter temperatures in the Sonoran Desert, but they could not adequately explain rain days. Our simulations demonstrate the complexities inherent to the climate influences on the desert southwest, as ice symmetry and tropical SSTs interacted with each other to influence the climate system. El Niño, in general, can significantly increase winter precipitation in the southwest [*Cayan and Peterson,* 1989; *Douglas and Englehart*, 1981] but we must also consider how this study demonstrates that ENSO-phase influences the degree of change that ice forcing can induce within the climate system (figures 1,2,3), and this influence could have ramifications for the prediction of future climate states and precipitation regimes in the desert southwest.

Ravelo at al. [2006] discuss the persistent El Niño climate state experienced during the warm Pliocene, and Federov et al. [2006] express that future climate change could induce early Pliocene-like conditions, which would then feature perennial El Niños. In our simulations, increased ice combined with El Niño SSTs produced the smallest changes in storm tracks and precipitation patterns for the desert southwest as compared to modern ice conditions under similar SSTs. Strong El Niño conditions combined with future reductions in sea ice may not produce the substantial degree of drying in the desert

southwest expressed by some modeling studies [*Sewall and Sloan*, 2004; *Sewall*, 2005; *Singarayer et al.*, 2006]. The response of climate to reduced sea ice extent may be very different than expected under perennial El Niño conditions. Future climate predictions need to explore how potential changes in periodicity and intensity of modes of variability, such as ENSO, interact with climate altered surface forcing. Differing ENSO-phases and their strength and duration may have significant impacts on projected future climate changes, and these changes in precipitation, evaporation, and storms could have far-reaching consequences in terms of water availability for the desert southwest.

Conclusions

Increased Arctic sea ice forcing at a scale similar to conditions experienced during the Little Ice Age can influence winter precipitation regime and storminess in the desert southwest. However, by exerting control on atmospheric structure, ENSO-phase influences the degree to which ice forcing can impact southwestern climate. High latitude atmospheric structure under ENSO-Neutral SST conditions provides the best opportunity for Arctic sea ice forcing to influence mid-latitude storm tracks in Western North America by allowing for the greatest ice-related steepening of the Z_{500} gradient, which exerts control on the strength and location of the polar jet. The more zonal (less steep Z_{500} gradient) conditions occurring during El Nino are not particularly conducive to producing changes in atmospheric structure due to increased ice, and La Nina SSTs contributed to gradient changes falling between those of ENSO-Neutral and El Nino conditions.

This relative steepening of the Z_{500} gradient and the resultant impacts on highs/lows and the polar jet, influence mid-latitude climate by altering patterns and intensity of precipitation and evaporation.

These altered patterns significantly affected winter climate in the desert southwest, and, within the southwest, response to increased Arctic sea ice differed with ENSO-phase. Increased ice and ENSO-Neutral SST conditions produced widespread increases in southwestern precipitation. La Nina and El Nino SSTs did not produce a widespread trend in precipitation in the southwest; instead these SST conditions contributed to both localized increases and decreases, which equated to a small average decrease in precipitation for the entire desert southwest region. Additionally, relative evaporation relationships to precipitation were altered with increased sea ice. In some locations, reductions in precipitation were paired with reductions in evaporation, such that the overall moisture loss was reduced. This indicates that exclusive of changes in precipitation, changes in relative evaporation can affect the total moisture budget in arid environments, such as the desert southwest, which may effectively function as a drought buffer/enhancer.

The symmetry of the Arctic sea ice anomaly is also a factor in influencing climate. Expansion of sea ice exhibits differing climate responses not only based upon amount of increase, but also the locations of expansion. Climate response in western North America and the desert southwest varied considerably between LIA and AS-LIA ice conditions; in some cases, the response for a given cell or small region was of opposite magnitude, such as with precipitation in central California in El Nino SST simulations. Responses to spatial differences in ice anomalies can occur both adjacent to locations of change, as described by Deser et al. [2000], but also can affect regions located far from the ice anomaly, such as the observed influence on storm tracks in the desert southwest in these simulations.

These findings suggest that the significant drying in the southwest predicted by modeling studies [*Sewall and Sloan*, 2004; *Sewall*, 2005; *Singarayer et al.*, 2006] must be considered alongside future predictions of modes of variability, such as ENSO. Some researchers have indicated that we may have strong or persistent El Nino conditions in the future, similar to the early Pliocene [*Fedorov et al.*, 2006], and these future El Nino conditions may reduce the potential degree of drying predicted under simulations that use more Neutral SST conditions. Further exploration of the interactions between ENSO and Arctic forcing may provide valuable insight into future precipitation regimes and storm tracks in the mid-latitudes under potential climate change scenarios.

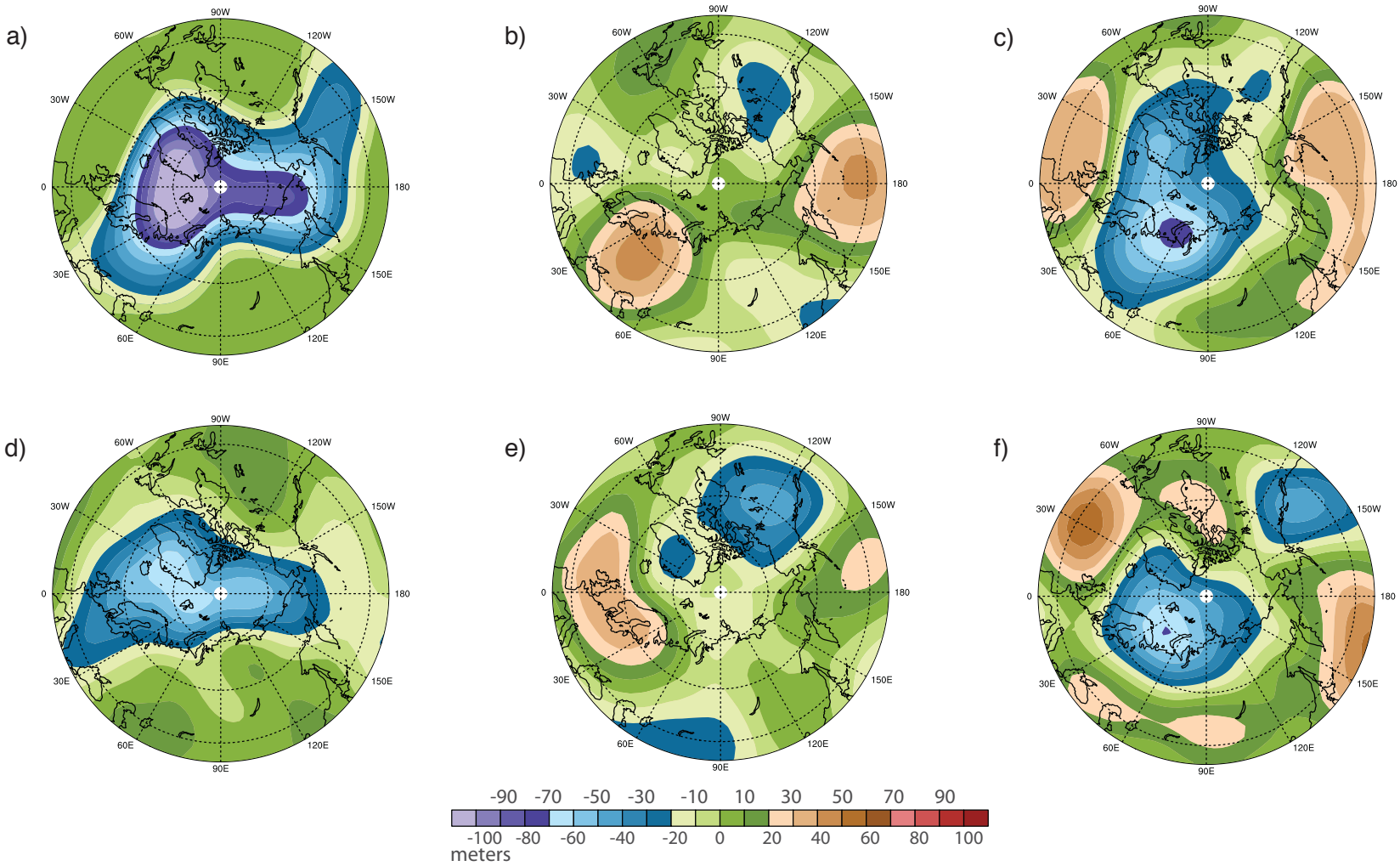

Figure 1: North polar projection plot showing winter (December, January, February) 500 mb geopotential height (Z_{500}) differences in meters (LIA or AS-LIA minus MOD) due to imposed increase in Arctic sea ice extent. LIA-Neutral compared to MOD (a) has the largest and most symmetrical anomalies with decreases throughout the high latitudes and small increases between 30-50° latitude. AS-LIA-Neutral (d) demonstrates a similar pattern with a smaller magnitude. LIA-Niña (c) and AS-LIA Niña (f) Z_{500} decreases are approximately centered over the Barents and Kara seas, with small increases (<5 meters) in Z_{500} seen over portions of the Atlantic Ocean between 30°N and 55°N and the Pacific Ocean south of 55°N. LIA-Niño (b) and AS-LIA-Niño (e) responses are much weaker with reductions of ~2-4 meters over North America and increases of ~2-4 meters over Europe and the Pacific Ocean, with relatively stronger decreases in AS-LIA-Niño, and relatively greater increases in LIA-Niño.

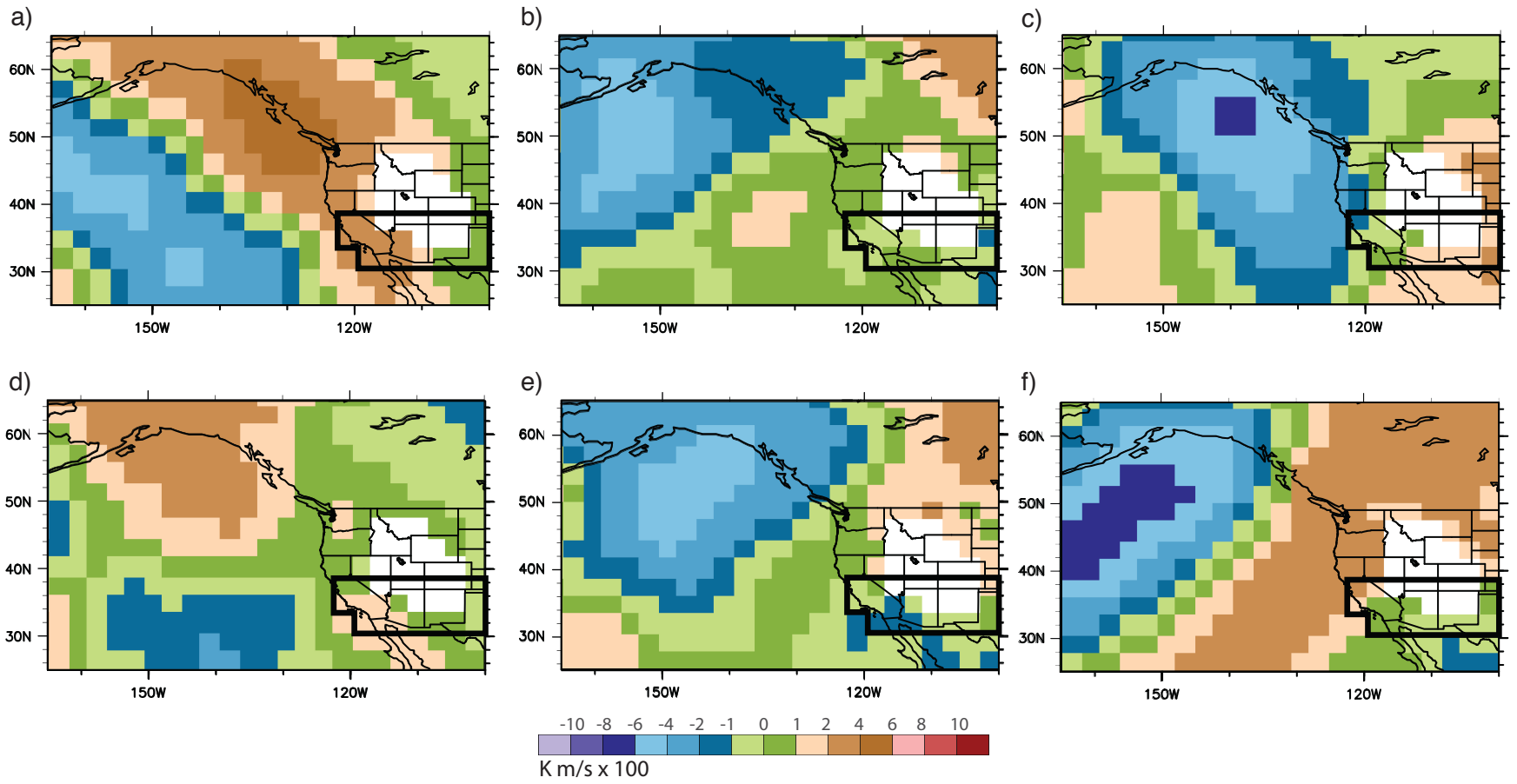

Figure 2: Winter (December, January, February) 850 mb meridional heat transport (VT850) differences (LIA or AS-LIA minus MOD) over western North America and highlighted desert southwest subregion due to imposed increase in Arctic sea ice extent. LIA-Neutral (a) features a relative increase in meridional heat transport penetrating into Western North America and parts of the desert southwest, and also represents an absolute change of 147% throughout Western North America and 323% in the desert southwest. AS-LIA-Neutral (d) shows less change over western North America (47%) and the desert southwest (126%). LIA-Niño (b) and AS-LIA-Niño (e) difference plots show the smallest absolute proportional change for Western North America (24% and 39%, respectively) and changes in the desert southwest are localized, centered over the Texas Panhandle in LIA-Nino and over Southern California in AS-LIA-Niño, with the average VT850 change in the desert southwest of 35% for LIA-Niño and 121% for AS-LIA-Niño. The greatest changes in LIA-Niña (c) and AS-LIA-Niña (f) occur over the Pacific Ocean, with much smaller changes over land and in the desert southwest. For western North America, LIA-Niña changes by 50% and AS-LIA-Niña by 44%, and over the desert southwest, 57% and 42%, respectively.

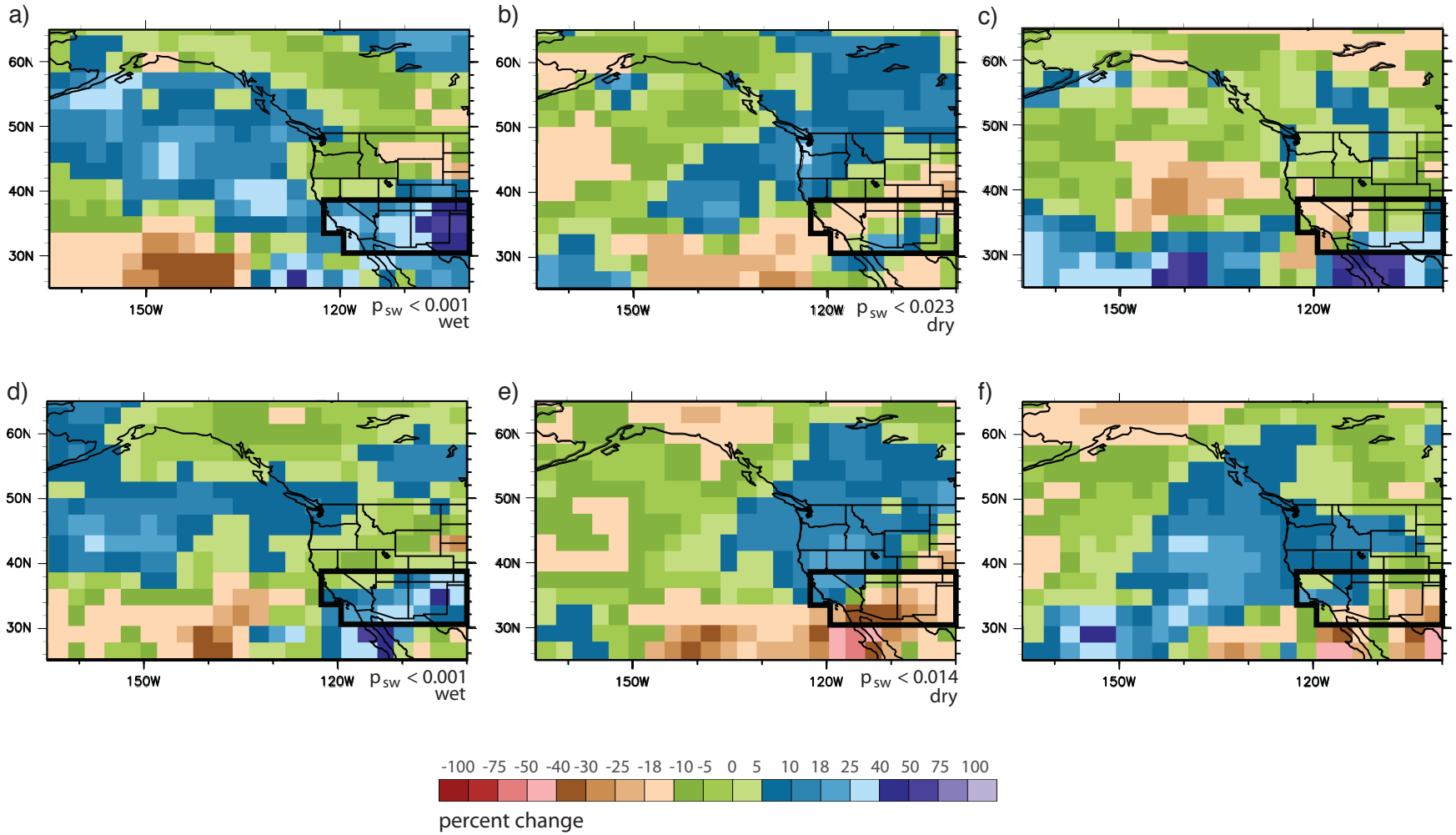

Figure 3: Winter (December, January, February) precipitation percent differences (LIA or AS-LIA minus MOD) due to imposed increase in Arctic sea ice extent. Percents calculated as (exp_cell-ctrl_cell/ctrl_cell x 100). Significant (α = 0.05) increases/decreases in desert southwest precipitation determined by a paired t-test on raw precipitation measurements are indicated by the reported p-value. The largest, most widespread precipitation increases in the desert southwest occur under LIA-Neutral (a) and AS-LIA-Neutral (d) conditions. Precipitation increases are generally smaller in magnitude and concentrated within smaller sections of the desert southwest and decreases in precipitation are more widespread in LIA-Niña (c), AS-LIA-Niña (f), LIA-Niño (b), and AS-LIA-Niño (e).

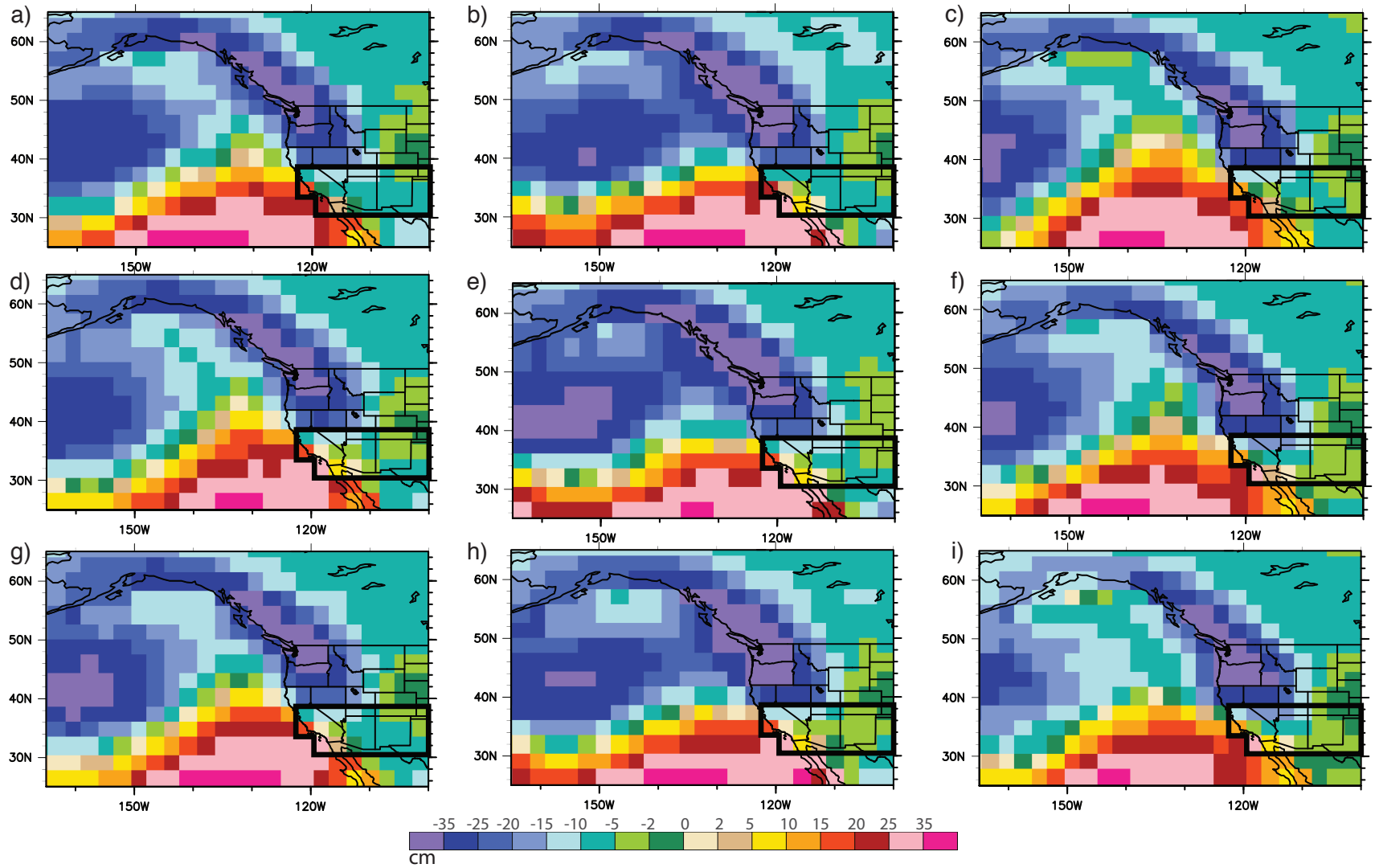

Figure 4: Winter (December, January, February) Evaporation minus Precipitation (E-P) actual values in centimeters over western North America and highlighted desert southwest sub-region due to imposed increase in Arctic sea ice extent. Significant ($\alpha = 0.05$) increases in moisture compared to MOD determined by a paired t-test measurements are indicated by the reported p-value. Cooler colors (negative values) indicate greater total moisture. Both LIA-Neutral (a, $p = 0.001$) and AS-LIA-Neutral (g, $p < 0.001$) show greater moisture as compared to MOD-Neutral (d). Smaller moisture increases are seen in LIA-Niño (b, $p = 0.047$) (as compared to MOD-Niño (e)) and LIA-Niña (c) (as compared to MOD-Niña(f)). AS-LIA-Niño (h) and AS-LIA-Niña (i) generally show reductions in moisture in the desert southwest as compared to MOD-Niño (e) and MOD-Niña (f), respectively.

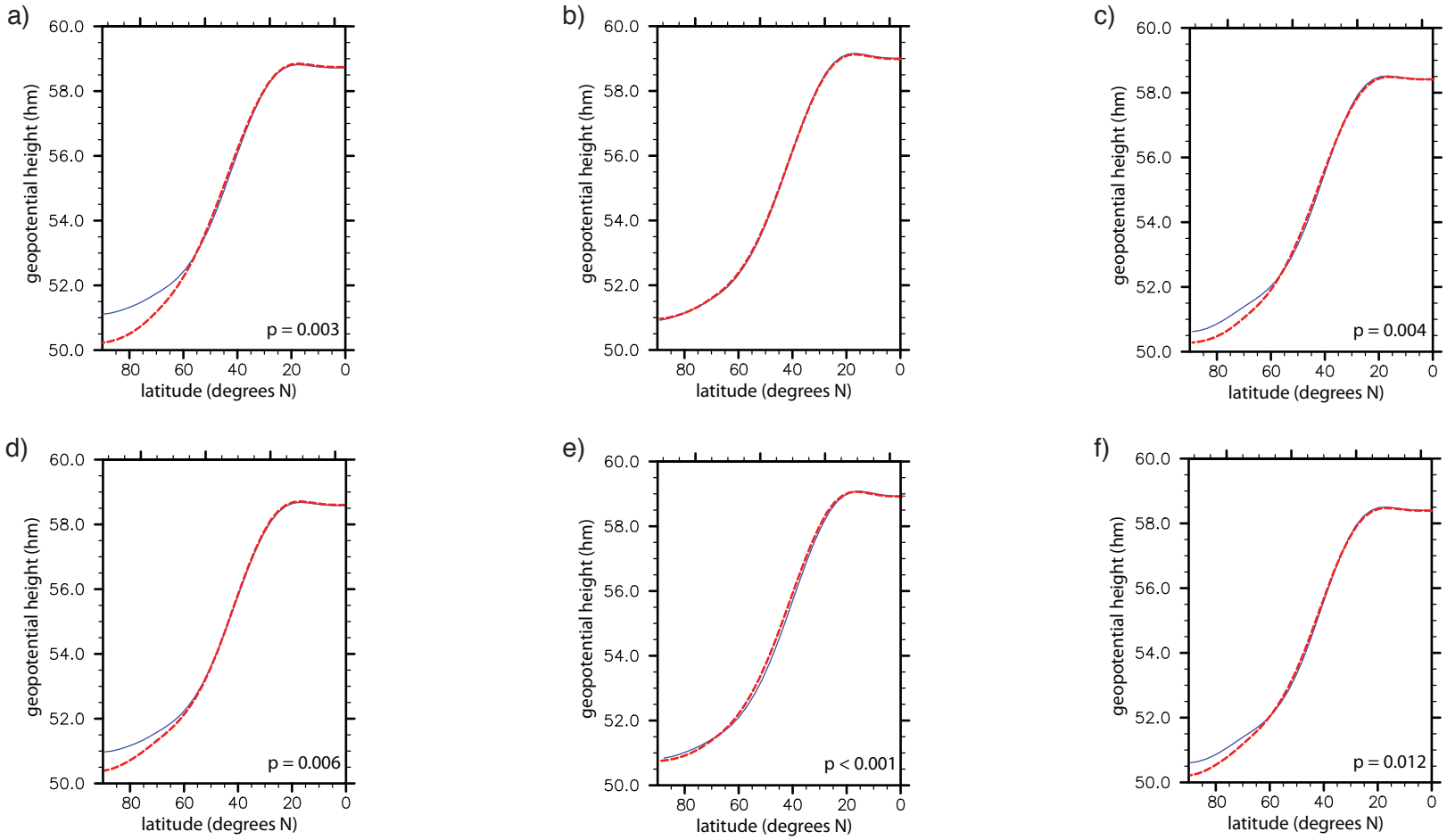

Figure 5: Winter (December, January, February) 500 mb geopotential height average by latitude in the Northern Hemisphere for both MOD and expanded Arctic Sea Ice (LIA, AS-LIA). 2-tailed significance from paired t-tests at the $\alpha = 0.05$ level indicated by the the p-value adjacent to each plot . Each plot features both Experimental (LIA, AS-LIA) values for a given ENSO member (Neutral, Niño, Niña) in red and MOD values in blue. LIA-Neutral (a), LIA-Niña (c), AS-LIA-Neutral (d), and AS-LIA-Niña (f) visibly deviate from their MOD counterparts, creating a stronger geopotential height gradient. LIA-Niño (b) and AS-LIA-Niño (e) show much less deviation from MOD. The changes in atmospheric structure indicated by the steepening of the geopotenial height gradient have the potential to alter storm tracks.

References

Barry, R. G., and R. J. Chorley (1998), *Atmosphere, weather and climate*, 7 ed., Routledge, London.

Bradley, R. S., and P. D. Jones (1992), *Climate since A. D. 1500*, 679 pp.

Briffa, K. R., and P. D. Jones (1991), Tree-Ring Density Reconstructions of Summer Temperature Patterns across Western North America since 1600, *Journal of Climate*, *5*(July), 735-754.

Briffa, K. R. (2000), Annual climate variability in the Holocene: interpreting the message of ancient trees, *Quaternary Science Reviews 19*(1-5), 87-105.

Brinck Løyning, T., et al. (2003), ACSYS Historical Ice Chart Archive (1553-2002), World Climate Research Program, Tromsø.

Bryson, R. A., and F. K. Hare (1974), The climates of North America, in *World Survey of Climatology, Climates of North America*, edited by R. A. Bryson and F. K. Hare, pp. 1-47, Elsevier, New York.

Castiglia, P. J., and P. J. Fawcett (2005), Large Holocene lakes and climate change in the Chihuahuan Desert *Geology*, *34*(2), 113-116.

Cayan, D. R., and D. H. Peterson (1989), The influence of north Pacific atmospheric circulation on streamflow in the west, *Geophysical Monograph*, *55*, 375-397.

Cayan, D. R., et al. (1999), ENSO and Hydrologic Extremes in the Western United States*, *Journal of Climate*, *12*(9), 2881-2893.

Christina Ravelo, A., et al. (2006), Evidence for El Niño-like conditions during the Pliocene, *GSA Today*, *16*(3), 4-11.

Cobb, K. M., et al. (2003), El Niño/Southern Oscillation and tropical Pacific climate during the last millennium, *Nature*, *424*(17 July), 271-276.

Comiso, J. C. (2002), A rapidly declining perennial sea ice cover in the Arctic, *Geophys. Res. Lett.*, *29*.

Comiso, J. C., et al. (2008), Accelerated decline in the Arctic sea ice cover, *Geophys. Res. Lett.*, *35*.

D'Arrigo, R., et al. (2005), On the variability of ENSO over the past six centuries , *Geophysical Research Letters*, *32*(2), L03711.

D'Arrigo, R. D., and G. C. Jacoby (1991), A 1000-year record of winter precipitation from northwestern New Mexico, USA: A reconstruction from tree-rings and its relation to El Niño and the Southern Oscillation, *The Holocene*, *1*, 95-101.

Deser, C., et al. (2000), Arctic Sea Ice Variability in the Context of Recent Atmospheric Circulation Trends, *Journal of Climate*, *13*(3), 617-633.

Douglas, A. V., and P. J. Englehart (1981), On a Statistical Relationship between Autumn Rainfall in the Central Equatorial Pacific and Subsequent Winter Precipitation in Florida, *Monthly Weather Review*, *109*(11), 2377-2382.

Fedorov, A. V., et al. (2006), The Pliocene Paradox (Mechanisms for a Permanent El Nino), *Science*, *312*(5779), 1485-1489.

Francis, J. A., et al. (2009), Winter Northern Hemisphere weather patterns remember summer Arctic sea-ice extent, *Geophysical Research Letters*, *36*, L07503.

Gleick, P. H., and D. B. Adams (2000), Water: The Potential Consequences of Climate Variability and Change. A Report of the National Assessment, U.S. Global Change Research Program, U.S. Geological Survey, Oakland, California.
Grove, J. M. (1988), *The Little Ice Age*, Methuen, London.
Herweijer, C., et al. (2006), North American droughts of the mid to late nineteenth century: a history, simulation and implication for Mediaeval drought, *The Holocene*, *16*(2), 159-171.
Hidalgo, H. G. (2004), Climate precursors of multidecadal drought variability in the western United States, *Water Resour. Res.*, *40*.
Holland, M. M., et al. (2006), Future abrupt reductions in the summer Arctic sea ice, *Geophys. Res. Lett.*, *33*.
Jorgensen, D. L., and W. H. Klein (1967), A synoptic climatology of winter precipitation from 700-mb lows for intermountain areas of the West., *Journal of Applied Meteorology*, *6*, 782-790.
Lamb, H. H. (1963), Mapping methods applied to the study of climatic variations and vicissitudes, in *The Changing Climate, Selected papers by H.H. Lamb*, edited, Methuen & Co Ltd., London.
Lamb, H. H. (1976), Climate in Historical Times, in *Climate, present, past and future*, edited by H. H. Lamb, pp. 423-473, Methuen, London.
Legates, D. R., and C. J. Willmott (1990), Mean seasonal and spatial variability in gauge-corrected, global precipitation, *International Journal of Climatology*, *10*, 111 - 128.
Loik, M. E., et al. (2004), A multi-scale perspective of water pulses in dryland ecosystems: climatology and ecohydrology of the western USA *Oecologia*, *141*, 269-281.
Magnusdottir, G., et al. (2004), The Effects of North Atlantic SST and Sea Ice Anomalies on the Winter Circulation in CCM3. Part I: Main Features and Storm Track Characteristics of the Response, *Journal of Climate*, *17*(5), 857-876.
Mann, M. E., et al. (2005), Volcanic and Solar Forcing of the Tropical Pacific over the Past 1000 Years, *Journal of Climate*, *18*(3), 447-456.
Perry, M. J., and P. J. Mackun (2001), Population Changes and distribution: Census 2000 brief (C2KBR/01-2), edited by U. S. D. o. C. E. a. S. Administration, p. 7.
Rayner, N. A., et al. (2003), Global analyses of sea surface temperature, sea ice, and night marine air temperature since the late nineteenth century, *J. Geophys. Res.*, *108*.
Salzer, M. W., and K. F. Kipfmueller (2005), Reconstructed Temperature And Precipitation On A Millennial Timescale From Tree-Rings In The Southern Colorado Plateau, U.S.A, *Climatic Change*, *70*(3), 465-487.
Sewall, J. O., and L. C. Sloan (2004), Disappearing Arctic sea ice reduces available water in the American west *Geophysical Research Letters*, *31*, L06209 06201- 06204.
Sewall, J. O. (2005), Precipitation shifts over western North America as a result of declining Arctic sea ice cover: the coupled system response, *Earth Interactions*, *9*, 26-21 - 26-23.
Sheppard, P. R., et al. (2002), The climate of the US Southwest, *Climate Research*, *21*(July 16), 219-238.
Singarayer, J. S., et al. (2006), Twenty-First-Century Climate Impacts from a Declining Arctic Sea Ice Cover, *Journal of Climate*, *19*(7), 1109-1125.
Smedsrud, L. H., et al. (2008), Recent and future changes of the Arctic sea-ice cover, *Geophys. Res. Lett.*, *35*.

Walsh, J. E., and M. S. Timlin (2003), Northern Hemisphere sea ice simulations by global climate models, *Polar Research*, *22*(1), 75-82.
Winograd, I. J., et al. (1998), The relative contributions of summer and cool-season precipitation to groundwater recharge, Spring Mountains, Nevada, USA, *Hydrogeology Journal*, *6*, 77-93.
Wolter, K., and M. S. Timlin (1993), Monitoring ENSO in COADS with a seasonally adjusted principal component index, paper presented at 17th Climate Diagnostics Workshop (Norman, OK), US Department of Commerce, Norman, OK.
Wolter, K., and M. S. Timlin (1998), Measuring the strength of ENSO events - how does 1997/98 rank? *Weather*, *52*, 315-324.
Woodhouse, C. A., and D. Meko (1997), Number of Winter Precipitation Days Reconstructed from Southwestern Tree Rings, *Journal of Climate*, *10*(10), 2663-2669.